JOURNAL OF QUATERNARY SCIENCE (2020) **35**(7) 855–868 ISSN 0267-8179. DOI: 10.1002/jqs.3241

JQS Journal of Quaternary Science QRA Quaternary Research Association

A continuous tephrostratigraphic record from the Labrador Sea spanning the last 65 ka

SUNNIVA RUTLEDAL,[1]* HAFLIDI HAFLIDASON,[1] SARAH M. P. BERBEN,[1] LISA GRIEM[1] and EYSTEIN JANSEN[1,2]
[1]Department of Earth Science, University of Bergen and Bjerknes Centre for Climate Research, Bergen, Norway
[2]Norwegian Research Centre (NORCE), Bergen and Bjerknes Centre for Climate Research, Bergen, Norway

Received 2 April 2020; Revised 10 August 2020; Accepted 13 August 2020

ABSTRACT: Volcanic ash preserved in marine sediment sequences is key for independent synchronization of palaeoclimate records within and across different climate archives. Here we present a continuous tephrostratigraphic record from the Labrador Sea, spanning the last 65–5 ka, an area and time period that has not been investigated in detail within the established North Atlantic tephra framework. We investigated marine sediment core GS16-204-22CC for increased tephra occurrences and geochemically analysed the major element composition of tephra shards to identify their source volcano(es). In total we observed eight tephra zones, of which five concentration peaks show isochronous features that can be used as independent tie-points in future studies. The main transport mechanism of tephra shards to the site was near-instantaneous deposition by drifting of sea ice along the East Greenland Current. Our results show that the Icelandic Veidivötn volcanic system was the dominant source of tephra material, especially between late Marine Isotope Stage (MIS) 4 and early MIS 3. The Veidivötn system generated volcanic eruptions in cycles of ca. 3–5 ka. We speculate that the quantity of tephra delivered to the Labrador Sea was a result of variable Icelandic ice volume and/or changes in the transportation pathway towards the Labrador Sea.

KEYWORDS: marine tephra; North Atlantic; Quaternary; tephra isochrons; tephrochronology

Introduction

Tephra (volcanic ash) shards ejected from volcanoes are deposited over large geographical areas in different sedimentary settings and can act as regional time-parallel marker horizons. The often geochemically distinct signature of tephra shards allows tracing of the source volcanic system and, in some cases, the specific eruption event from which the shards originate. Geochemically distinctive tephras embedded in marine sediment sequences have potential to be utilized as a reliable correlational tool in dating and synchronization of palaeoclimatic events within the marine realm, but also across different climate archives (e.g. Haflidason *et al.*, 2000; Lowe, 2011; Berben *et al.*, 2020). Marine tephrochronology is especially useful as marine sediment sequences are long and continuous and record clear climate signals simultaneously, both regionally and globally.

The established North Atlantic marine tephra framework spanning the Last Glacial period (LGP) [hereafter defined as Marine Isotope Stage (MIS) 5–2 (Rasmussen *et al.*, 2014)] includes significant widespread tephra horizons such as Faroe Marine Ash Zones (FMAZ) II–IV and North Atlantic Ash Zone (NAAZ) II (Haflidason *et al.*, 2000; Wastegård *et al.*, 2006; Griggs *et al.*, 2014; Abbott *et al.*, 2018a). In addition, with the recent advances in cryptotephra (tephra invisible to the naked eye) analysis (Davies, 2015), new tephra horizons, particularly from sites in the eastern North Atlantic (Abbott *et al.*, 2016, 2018a) and Nordic Seas (Griggs *et al.*, 2014; Berben *et al.*, 2020) have been reported. These recently discovered tephra deposits are predominantly of Icelandic origin and occur stratigraphically between Heinrich events (H) 4 and 3 (ca. 40 and 31 ka, respectively). They indicate an increase in Icelandic volcanic activity during this time interval. Spanning a longer time period, from ca. 86 to 12 ka, at least 78 tephra deposits have been identified in the northern Denmark Strait, with increased volcanic activity during the periods ca. 40–37 ka and ca. 56–50 ka (Voelker and Haflidason, 2015). Hence, there is an enormous potential to uncover tephra deposits in marine regions both distal and proximal to Iceland.

Due to the predominant strong westerlies, the prevailing direction for windblown ash from Iceland is eastwards (Haflidason *et al.*, 2000; Lacasse, 2001). Therefore, previous marine tephrochronological studies have mainly focused on these downwind regions east of Iceland. The synchronization of marine records across the wider North Atlantic requires the exploration of marine sediments in the western sector, which was the motive for investigation of the tephrochronological potential of the Labrador Sea reported here. This locality is key for monitoring palaeoclimatic shifts between the Nordic Seas, the east North Atlantic and the west North Atlantic (Griem *et al.*, 2019). Tephra deposits from this region dating to the LGP have been reported previously (Kvamme *et al.*, 1989; Wastegård *et al.*, 2006; Hesse and Khodabakhsh, 2016), but here we report the first continuous tephrostratigraphic record with comprehensive geochemical fingerprinting, an essential step for aligning marine records from the Labrador Sea to other North Atlantic marine records and the Greenland ice-core records.

The objective of this study is to provide a continuous tephra record from the Labrador Sea spanning the period 65–5 ka, and particularly the time interval ca. 65–30 ka. This objective has been achieved by using geochemical characteristics to link tephra layers to Icelandic volcanic systems and to already established tephra isochrons within the North Atlantic marine

*Correspondence: S. Rutledal, as above.
E-mail: sunniva.rutledal@uib.no

tephra framework and the Greenland ice-core tephra lattice (Bourne *et al.*, 2013, 2015; Griggs *et al.*, 2014; Wastegård and Rasmussen, 2014; Voelker and Haflidason, 2015; Abbott *et al.*, 2016, 2018a).

Materials and methods

Marine sediment core

In this study, marine sediment core GS16-204-22CC, retrieved during the ice2ice-2016 cruise aboard R/V *G. O. Sars*, was investigated for potential existence of tephra deposits. This calypso sediment core was taken from the eastern Labrador Sea, south of Greenland (58°02.83′N, 47°02.36′W) at 3160 m water depth (Fig. 1A). The marine sediment core is 1964 cm long and spans the early Holocene to approximately late MIS 6 (Griem *et al.*, 2019). The general lithology varies between grey silty clay and sandy silt (Dokken and Cruise-members, 2016). Previously, Griem *et al.* (2019) reported high-resolution stable isotope records measured on planktonic foraminifera *Neogloboquadrina pachyderma* (*N. pachyderma*) and ice-rafted debris (IRD) from this core (Fig. 2).

Chronology

An age model for core GS16-204-22CC has been presented by Griem *et al.* (2019). This age model is based on the tuning of planktonic $\delta^{18}O$ and $\delta^{13}C$ time series between core GS16-204-22CC and core PS2644-5 from the northern Denmark Strait (Voelker *et al.*, 1998). In addition, the identified rhyolitic component of Vedde Ash [12 171 ± 57 b2k (Svensson *et al.*, 2008)] (this study, Supporting information Fig. S1) and NAAZ II (II-RHY-1) [55 380 ± 1184 b2k (Svensson *et al.*, 2008)] (Griem *et al.*, 2019; Rutledal *et al.*, 2020) were used as independent time-markers. In total, the chronology is based on 10 tuning points, two accerlator mass spectrometry (AMS) ^{14}C dates and two tephra markers (Supporting Information Table S1). For the time period 65–25 ka, the average sedimentation

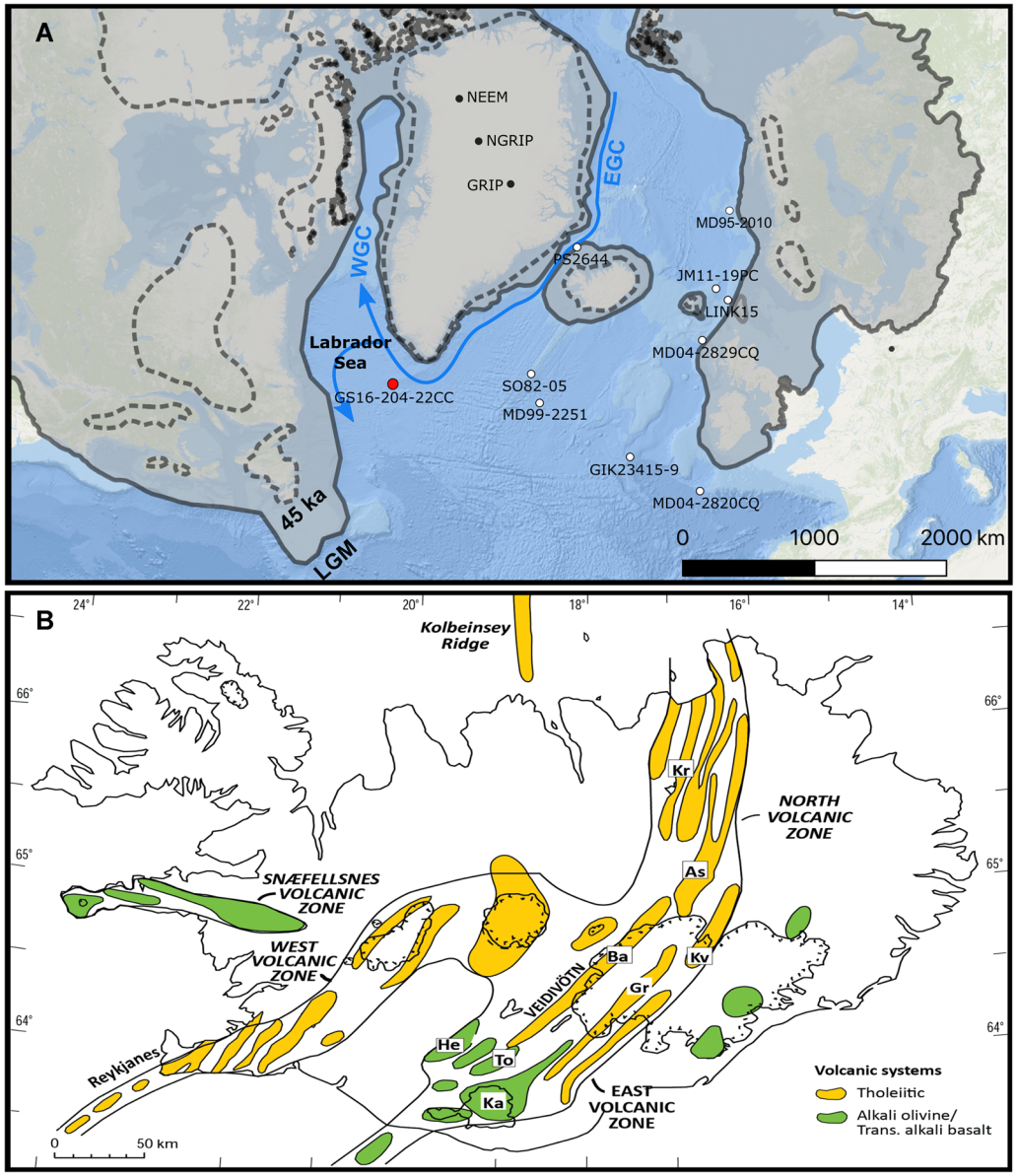

Figure 1. A: Map of the study region. The location of the marine sediment core GS16-204-22CC is marked by a red dot. The ice sheet extents of northern hemisphere ice sheets during the Last Glacial Maximum (LGM) (solid line) and ca. 45 ka b2k (dotted line) are shown by grey shading after Batchelor *et al.* (2019). The locations of marine sediment and ice cores referenced in the text are marked by white and black dots. WGC = West Greenland Current, EGC = East Greenland Current, JM = Jan Mayen. Basemap by ESRI Ocean. B: The main volcanic systems on Iceland (modified from Haflidason *et al.*, 2000). As = Askja, Ba = Bárdarbunga-Veidivötn, Gr = Grímsvötn, He = Hekla, Ka = Katla, Kr = Krafla, Kv = Kverkfjöll, To = Torfajökull. [Color figure can be viewed at wileyonlinelibrary.com]

rate is 8.5 cm ka^{-1}. Hence, ~230 years separate each analysis when analysed with a 2-cm spacing. In addition, with a sample width of 0.5 cm, each sample represents ~50 years. Here, the age model established for core GS16-204-22CC is predominantly used as a tool to provide a chronological context for the identified tephra deposits, and thus aid in their potential geochemical correlation to established tephra deposits in the literature. For a more detailed description of the GS16-204-22CC chronology, we refer the reader to Griem *et al.* (2019).

Tephra analysis

The sediment core sequence between 0 and 540 cm was investigated for tephra occurrences. First the section between 0 and 190 cm was continuously investigated every 5 cm and the section between 190 and 540 cm every 2 cm, in the grain size fraction 150–500 μm. Intervals of elevated tephra shard concentrations were further investigated in the grain size fractions 106–150 and 63–106 μm. These specific size fractions are the result of previously published IRD and foraminiferal concentration records (Griem *et al.*, 2019). Tephra shards were counted using the same technique as for IRD counting. Here the sample is divided into equal parts using a sample splitter (Feyling-Hanssen, 1971), until a minimum of 300 grains are left for counting under an optical microscope. Depth intervals with elevated tephra shard concentrations were chosen for geochemical analysis. From the selected depth intervals, tephra shards were carefully extracted and placed onto frosted microscope slides and eventually embedded in epoxy resin following previously published methodologies (Abbott *et al.*, 2011, 2018b; Griggs *et al.*, 2014). To expose the glass shards, the mounted tephra material was carefully ground on p1000 silicon carbide paper and polished using ¼ diamond polycrystalline suspension. Single tephra shards were analysed using electron-probe microanalysis (EPMA) at the Tephrochronological Analysis unit, University of Edinburgh. A Cameca SX100 with five vertical wavelength dispersive spectrometers provided oxide values (wt.%) of 10 major elements from each measured tephra shard. Following the protocols outlined in Hayward (2012), ~10–40 shards were analysed for each sample. Totals <97 wt.% were rejected. We used a beam size of 5 μm for all analyses. In addition, to ensure analytical precision, secondary standards [BCR2g (Basalt) and Lipari Obsidian (Rhyolitic)] were measured at the start and end of each run.

The major element data obtained from each tephra deposit were graphically examined and statistically compared to previously published marine and ice-core tephra horizons dating to the same time period using similarity coefficient (SC) and statistical distance (SD) tools (Borchardt *et al.*, 1972; Perkins *et al.*, 1995). Davis (1985) suggests that SC values between 0.95 and 1 indicate identical datasets. However, due to great similarity among the Icelandic volcanic systems and the products of individual volcanic systems, Abbott *et al.* (2018a) suggest that only SCs >0.97 represent identical datasets. While the SC considers how similar two datasets are, the SD function estimates the differences between datasets. The SD values are compared to critical values at a 99% confidence interval, which is 18.48 for rhyolitic material and 23.21 for basaltic material. The rhyolitic and basaltic values differ because major element comparisons are based only on those elements recording (averaged) values >0.1 wt.% (10 elements for basaltic material and seven elements for rhyolitic material). SD values larger than the critical value at a 99% confidence interval [i.e. 18.48 (rhyolitic) and 23.21 (basaltic)] suggest two different datasets, but lower values do not indicate identical datasets (Pearce *et al.*, 2008).

Volcanic source identification

Iceland consists of four volcanic zones: the North, East, West and Reykjanes volcanic zones (NVZ, EVZ, WVZ and RVZ) (Fig. 1B) (Thordarson and Larsen, 2007). These volcanic zones are further separated into 30 volcanic systems. Based on occurrences of tephra shards in Greenland ice-cores and marine sediment cores, the volcanic systems Katla, Hekla, Bárdarbunga-Veidivötn (hereafter Veidivötn), Grímsvötn, Kverkfjöll, Torfajökull and Reykjanes are considered the most active systems during the LGP (Fig. 1B) (e.g. Haflidason *et al.*, 2000; Bourne *et al.*, 2013, 2015; Voelker and Haflidason, 2015; Abbott *et al.*, 2016, 2018a). To identify the volcanic source of the tephra deposits recorded in GS16-204-22CC, we compared their geochemical composition to those of Icelandic volcanic systems using the database of Harning *et al.* (2018) and references therein. The former is based on modern to Holocene geochemistry of the volcanic systems. However, the geochemistry of volcanic systems evolves with time, and knowledge of the geochemical properties of these systems during the LGP is limited (Voelker and Haflidason, 2015). Therefore, there are uncertainties in the linkage of deposits to known volcanic systems when working with pre-Holocene tephra. This is especially true for the geochemically very similar Veidivötn and Reykjanes volcanic systems, as well as the Kverkfjöll and Grímsvötn volcanic systems.

Evaluating the isochronous integrity of tephra deposits

We evaluated the isochronous integrity of each tephra zone using the tephra deposit classification scheme outlined by Abbott *et al.* (2018b). Those relevant for this study are the Type 2A, 2B and 3 deposits. A Type 2 deposit is characterized by a distinct peak in shard concentration (100 s to 1000 s of shards per 0.5 g dry weight), with an upward and downward span of shards on either side of the main concentration peak. If the deposit is homogeneous it is characterized as a Type 2A deposit and was probably transported by sea ice or primary airfall. If the deposit is heterogeneous it is characterized as a Type 2B deposit and was probably transported by iceberg rafting. A Type 3 deposit has a flat-bottomed profile with an upward tail of shards caused by bioturbation and other secondary depositional mechanisms. The main concentration peak is homogeneous, and the most likely transportation mechanism was sea ice rafting or primary airfall. For most marine tephra deposits the main concentration peak is interpreted to represent the tephra isochron. However, post-depositional processes such as bioturbation and bottom-current reworking might increase the vertical spread of the deposit and mask the main concentration peak (Abbott *et al.*, 2018b). In such cases, providing a depth/age range for the tephra deposit might be more appropriate. In addition, we acknowledge that the term 'isochronous' should be taken with caution as one tephra deposit can cover 100 s of years due to low sedimentation rates and age model uncertainties.

During the LGP, large continental ice sheets such as the Greenland Ice Sheet (GIS), the Laurentide Ice Sheet (LIS) and Icelandic Ice Sheet (IIS) influenced the study site (Fig. 1A). However, the extents of these ice sheets have varied through time. For example, the LIS was much larger during the Last Glacial Maximum (LGM) compared to the period ca. 45–40 ka (Batchelor *et al.*, 2019) (Fig. 1A). The growth and decay of

continental ice sheets are reflected in the marine IRD record as icebergs act as the primary transport agent for IRD. Hence, at the core site, an increased occurrence of IRD indicates additional iceberg transport and melt. In addition to lithic material, icebergs also transport tephra shards that have been incorporated in the ice for up to several millennia (Brendryen *et al.*, 2010). This time delay between the volcanic eruption, iceberg calving and subsequent deposition on the ocean floor will compromise the isochronous integrity of the tephra deposit. Through the LGP, the GS16-204-22CC IRD record is characterized by a continuous IRD input, which indicates that icebergs were within the proximity of the study site at all times (Griem *et al.*, 2019). Therefore, we evaluate the combined record of IRD, geochemical composition and stratigraphic appearance signals when determining the transport mechanism of each tephra zone.

Tephrostratigraphy

The tephrostratigraphic record of GS16-204-22CC, spanning the period from ca. 65 to 5 ka, is based on 10 recorded levels of increased tephra shard concentrations (Fig. 2A,B). In the following text we define these levels as 'tephra zones (TZ)'. The most pronounced tephra deposits are recorded at 130–130.5 and 474–474.5 cm. The 130–130.5 cm layer represents the rhyolitic Vedde Ash tephra and the 474–474.5 cm layer NAAZ II (II-RHY-1) (Griem *et al.*, 2019; Rutledal *et al.*, 2020) (Supporting Information Fig. S1). Both horizons are in this study solely utilized as chronological tie-points, and hence not discussed further (see 'Chronology'). The remaining eight recorded tephra deposits are analysed here in terms of their shard profiles and concentration peaks, their geochemical composition, and any co-occurrence of IRD. The last of these is investigated to assess their (most likely) deposit type, transportation mechanism and volcanic source.

Tephra zone 1 (TZ-1): GS16-204-22CC, 530.25–524.25 cm (ca. 64.3–63.7 ± 0.5 ka b2k)

A stratigraphic level of increased tephra shard concentrations is identified between 530.25 and 524.25 cm. At 530.25 cm core depth, a clear tephra concentration peak is observed in all size fractions (Fig. 2A,B). This core depth has, according to the age model (Griem *et al.*, 2019), an age estimate of ca. 64.3 ± 0.5 ka b2k (Supporting Information Fig. S2). From the concentration peak, basaltic tephra material (150–500 and 63–106 µm), including a tuff fragment ca. 1.5 cm in diameter, was geochemically analysed. In addition, basaltic shards from a smaller concentration peak recorded at 524.25 cm, about 600 years

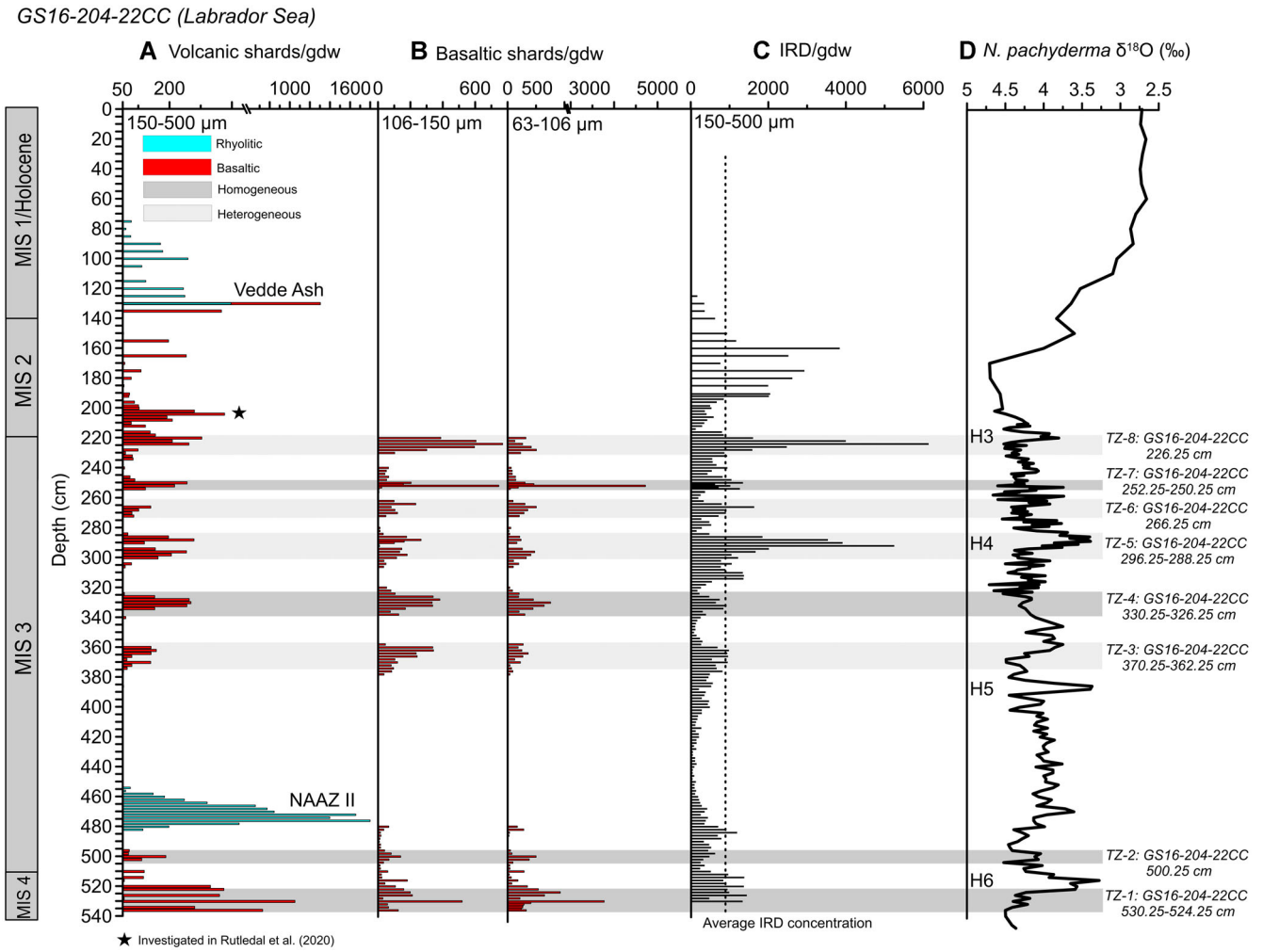

Figure 2. Tephrostratigraphic record from Labrador Sea core GS16-204-22CC, 0–540 cm versus depth (cm). (A) Occurrence of volcanic shards (basaltic and rhyolitic)/gram dry weight (gdw), 150–500 µm. (B) Occurrence of basaltic shards/gram dry weight (gdw), 106–150 µm and 63–106 µm. Please note that basaltic shards/gdw were only counted for selected intervals (i.e. TZ 1–8). (C) IRD (ice-rafted debris)/gdw from the size fraction 150–500 µm (Griem *et al.*, 2019). (D) $\delta^{18}O$ isotope record of the planktic foraminifera *N. pachyderma* (Griem *et al.*, 2019). Grey vertical bars mark the eight tephra zones described in the text, whereas Vedde Ash and NAAZ II are indicated by name. Vertical dotted line marks the average IRD concentration within the sediment core. H3–H6 = Heinrich events 3–6.

later in the record, at ca. 63.7 ± 0.5 ka b2k (Fig. S2a), was analysed to assess its relationship with the underlying peak at 530.25 cm. The analysed material from both depth intervals shows a fairly homogeneous basaltic composition (Fig. 3A) and a geochemical affiliation with the Veidivötn volcanic system in the EVZ (Harning *et al.*, 2018) (Fig. 4A,E). For this time period, there are no reports of a Veidivötn eruption in either the Greenland ice-core records or the North Atlantic marine tephra framework (e.g. Brendryen *et al.*, 2010; Bourne *et al.*, 2015; Abbott *et al.*, 2018a). The TZ-1 tephra shard concentration peak is a distinct single peak in both the coarse- and the fine-grained fractions, indicating a Type 2A deposit (Abbott *et al.*, 2018b). The tephra deposit co-occurs with increased IRD concentrations (Fig. 2C). However, because iceberg deposits often exhibit a heterogeneous geochemistry, this transport mechanism is considered unlikely. Instead, the combination of fairly homogeneous geochemistry and relatively high abundance of coarse-grained tephra indicates a near-instantaneous deposition of this tephra layer by drifting sea ice. The tephra shards were probably transported westwards off the Icelandic continental shelf by air, and then southwards by drifting sea ice along the East Greenland Current (EGC). This is in line with suggestions of an enhanced arctic export and strong EGC in this time interval (Griem *et al.*, 2019). The tephra concentration peak identified at 600 years later (524.25 cm) is stratigraphically less defined but shows the same geochemistry as the underlying peak at 530.25 cm. This tephra peak could have originated from either a later volcanic eruption from the same active system or reworking of material from the older and underlying deposit.

Tephra zone 2 (TZ-2): GS16-204-22CC, 500.25 cm (ca. 58.1 ± 0.8 ka b2k)

At the level of 500.25 cm (Fig. 2A,B) and an estimated age of ca. 58.1 ± 0.8 ka b2k (Supporting Information Fig. S2), a distinct peak in volcanic material is recorded. Tephra shards from the grain size fractions 150–500 and 63–106 µm show a homogeneous basaltic population in both grain sizes (Fig. 3A) with a geochemical composition affiliated to the Veidivötn volcanic system located in the EVZ (Harning *et al.*, 2018) (Fig. 4B,F). This geochemical spectrum does not resemble any established tephra horizons within the Greenland ice-core tephra lattice or the North Atlantic tephra framework (e.g. Wastegård *et al.*, 2006; Bourne *et al.*, 2015; Abbott *et al.*, 2018a). TZ-2 occurs as an abrupt increase of tephra shards compared to background levels, with some up- and downward tailing of tephra shards. The tephra shards in the concentration peak show a homogeneous geochemistry, indicative of a Type 2A deposit (Abbott *et al.*, 2018b). The tephra zone does not accord with any increased levels of IRD (Fig. 2C). Due to the high concentration of relatively coarse-grained shards and homogeneous geochemistry, the tephra shards were probably transported and deposited near-instantaneously by drifting sea ice, in a similar manner as proposed for TZ-1 (ca. 6200 years older) and may be useful as a correlational tie-point for future studies.

Tephra zone 3 (TZ-3): GS16-204-22CC, 370.25–362.25 cm (ca. 46–45.3 ± 0.5 ka b2k)

Increased levels of tephra shards are observed in the interval between 370.25 and 362.25 cm (Fig. 2A), corresponding to an age estimate of ca. 46–45.3 ± 0.5 ka b2k (Supporting Information Fig. S2). Hence, the tephra shards were deposited shortly after H5 (Fig. 2d) and span a period of ca. 700 years (Fig. S2). Basaltic material (150–500 µm) from the tephra layer was geochemically analysed and showed a heterogeneous composition (Fig. 3B) with a predominantly Grímsvötn origin (Fig. 4C,G; Table 1), but 55% of the shards were collectively derived from the Katla, Hekla, Veidivötn (EVZ) and Kverkfjöll (NVZ) volcanic systems (Harning *et al.*, 2018). No tephra from the Katla, Hekla or Veidivötn volcanic systems is recorded in the Greenland ice-cores or North Atlantic marine tephra framework over this time period (e.g. Wastegård *et al.*, 2006; Bourne *et al.*, 2015; Voelker and Haflidason, 2015; Abbott *et al.*, 2018a). However, one Grímsvötn tephra horizon, known as FMAZ IV (ca. 46.8 ka BP), is recorded within the North Atlantic marine tephra framework (Griggs *et al.*, 2014; Wastegård and Rasmussen, 2014; Abbott *et al.*, 2018a). To investigate the geochemical similarity between the TZ-3 Grímsvötn shards and the FMAZ IV deposit recorded within different marine sediment cores (Fig. 1A; Table 1), we calculated the SC and SD, the former ranging from 0.95 to 0.98 and the latter from 1.48 to 5.13 (Table 1),

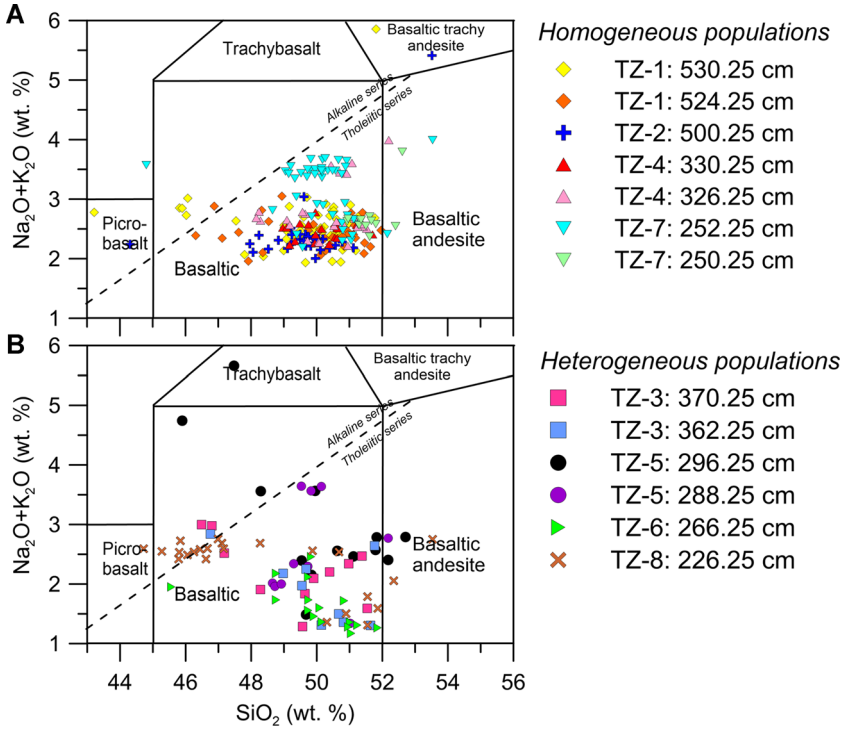

Figure 3 Total alkali silica (TAS) plot of the geochemical composition of tephra shards from GS16-204-22CC. A: Data from tephra zones with near-homogeneous composition (TZ 1, 2, 4, 7). B: Data from tephra zones with heterogeneous composition (TZ 3, 5, 6, 8). Chemical classification and nomenclature are from Le Maitre and Bateman (1989). [Color figure can be viewed at wileyonlinelibrary.com]

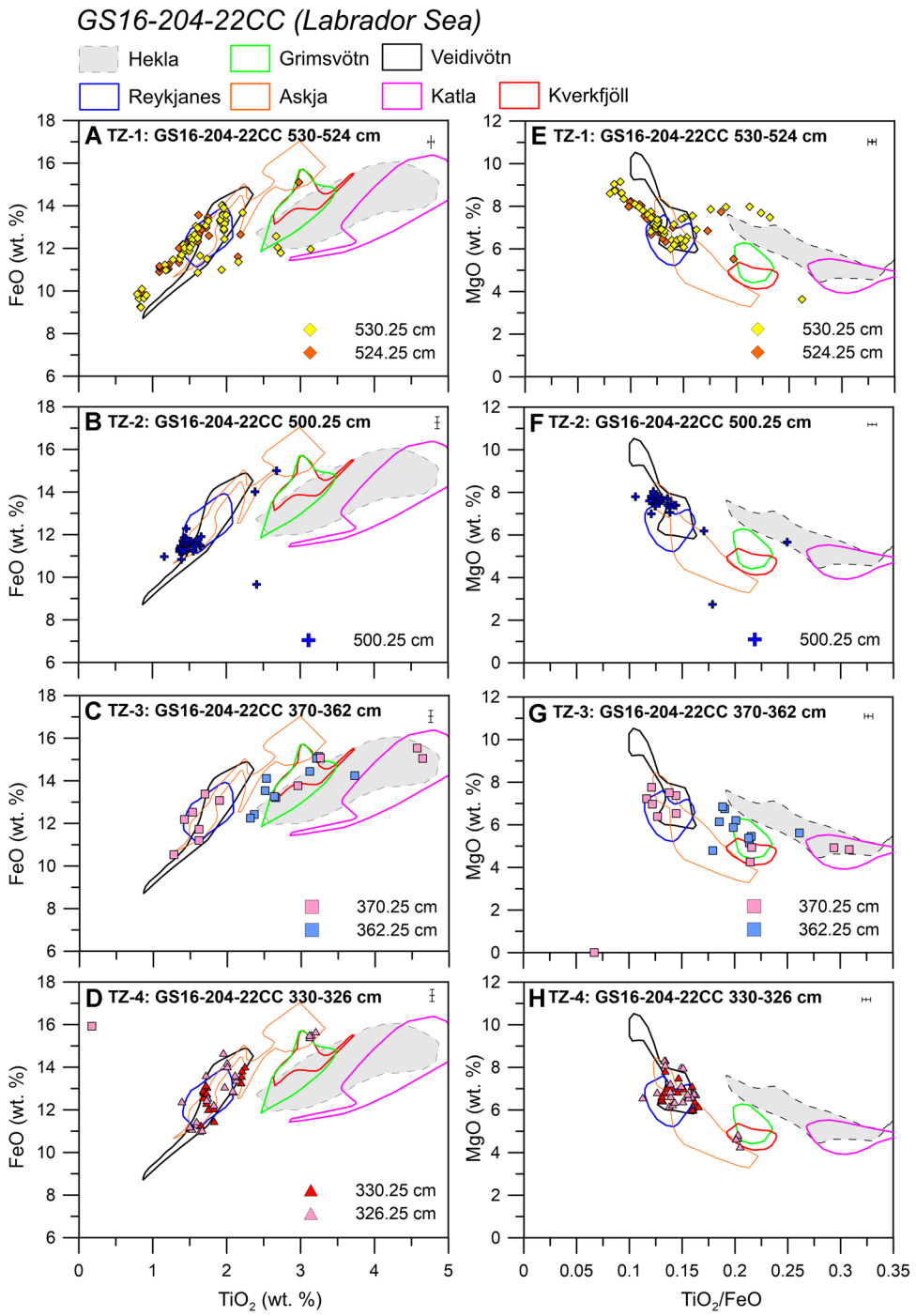

Figure 4. Visual biplot comparison (FeO versus TiO_2 and MgO versus TiO_2/FeO) of tephra shard analyses from marine sediment core GS16-204-22CC TZ 1–4. Geochemical envelopes of Icelandic volcanic systems after Harning *et al.* (2018). Error bars represent two standard deviations of replicate analysis of BCR2g reference glass. [Color figure can be viewed at wileyonlinelibrary.com]

indicating geochemical similarities that are also supported by the biplot graphics (Fig. 6A). We note that only geochemical data from Griggs *et al.* (2014) and Abbott *et al.* (2018a) were available for plotting, whereas statistical analysis was performed on data published by Griggs *et al.* (2014), Wastegård and Rasmussen (2014) and Abbott *et al.* (2018a). It is likely that the Grímsvötn tephra shards in TZ-3 originated from the same volcanic eruption(s) as the FMAZ IV deposit identified in multiple North Atlantic marine sediment cores (Griggs *et al.*, 2014; Wastegård and Rasmussen, 2014; Abbott *et al.*, 2018a). However, the transport mechanisms were different. The heterogeneous geochemistry of TZ-3, coupled with increased IRD concentrations (Fig. 2C), defines the deposit as a Type 2B deposit (Abbott *et al.*, 2018b), and the tephra grains were probably transported by icebergs over a period of ca. 700 years. Consequently, deposition of TZ-3 was delayed by comparison with FMAZ IV deposition in other records, which are reported as primary (near-instantaneous) deposits.

Tephra zone 4 (TZ-4): GS16-204-22CC, 330.25–326.25 cm (ca. 42.4–42.1 ± 0.5 ka b2k)

Between 330.25 and 326.25 cm (ca. 42.4–42.1 ± 0.5 ka b2k, Supporting Information Fig. S2), corresponding to a time span of ca. 300 years, a distinct basaltic tephra deposit is observed (Fig. 2A,B). The main concentration peak occurs at 330.25 cm (ca. 42.4 ± 0.5 ka b2k). Basaltic shards (150–500 µm) from core depths 330.25 cm (ca. 42.4 ± 0.5 ka b2k) and 326.25 cm

Table 1. Statistical comparison of the different geochemical populations from the GS16-204-22CC tephra layers with established horizons in the North Atlantic tephra framework and Greenland ice-core tephra lattice (Fig. 1A). References are as follows: a, Bourne *et al.* (2013, 2015); b, Abbott *et al.* (2018a); c, Abbott *et al.* (2016); d, Berben *et al.* (2020); e, Wastegård and Rasmussen (2014); f, Griggs *et al.* (2014); g, Lackschewitz and Wallrabe-Adams (1997).

GS16-204-22CC			GRIP[a]	NGRIP[a]	NEEM[a]	MD99-2251[b]	MD04-2829CQ[b]	MD04-2820CQ[c]	MD99-2284[d]	GIK23415 (302–306 cm)[b]	LINK15[e]	JM11-19PC 'FMAZ IV'[f]	MD95-2010 'FMAZ IV'[b]	SO82-05 'VZ 5'[g]
Tephra zone 1: GS16-204-22CC, 530–524 cm	Veidivötn (82%)	No match	–	–	–	–	–	–	–	–	–	–		–
	WVZ/RVB (10%)	No match	–	–	–	–	–	–	–	–	–	–		–
Tephra zone 2: GS16-204-22CC, 500.25 cm	Veidivötn (90%)	SC	–	–	–	–	–	–		–	–	–		–
		SD	–	–	–	–	–	–	–	–	–	–		–
	Hekla (3%)	No match	–	–	–	–	–	–	–	–	–	–		–
Tephra zone 3: GS16-204-22CC, 370–362 cm	Grimsvötn (35%)	**SC**	–	–	–	–	–	–	–	–	*347–348 cm* **0.97** *355–356 cm* **0.98**	**0.98**	**0.95**	**0.96**
		SD	–	–	–	–	–	–	–	–	*347–348 cm* **1.5** *355–356 cm* **5.13**	**2.11**	**3.49**	**1.97**
	Katla/Hekla? (17%)	No match	–	–	–	–	–	–	–	–	–	–		–
	Veidivötn (30%)	No match	–	–	–	–	–	–	–	–	–	–		–
	Kverkfjöll (8%)	No match	–	–	–	–	–	–	–	–	–	–		–
Tephra zone 4: GS16-204-22CC, 330–326 cm	Veidivötn (82%)	**SC**	–	–	–	–	–	*529–530 cm* **0.99**	–	–	–	–		–
		SD	–	–	–	–	–	*529–530 cm* **1.3**	–	–	–	–		–
	Kverkfjöll (9%)	**SC**	–	–	–	–	–	*524–525 cm* **0.98**	–	–	–	–		–
		SD	–	–	–	–	–	*524–525 cm* **3.12**	–	–	–	–		–
Tephra zone 5: GS16-204-22CC, 296–288 cm	Grimsvötn (26%)	**SC**	*2207 m* **0.98**	*2078.97 m* **0.97** *2079.40 m* **0.98** *2100.65 m* **0.98**	–	–	*930–931 cm* **0.964**	–	–	**0.98**	–	–		–

(*Continued*)

Table 1. (*Continued*)

GS16-204-22CC				GRIP[a]	NGRIP[a]	NEEM[a]	MD99-2251[b]	MD04-2829CQ[b]	MD04-2820CQ[c]	MD99-2284[d]	GIK23415 (302–306 cm)[b]	LINK15[e]	JM11-19PC 'FMAZ IV'[f]	MD95-2010 'FMAZ IV'[b]	SO82-05 'VZ 5'[g]
			SD	*2207 m* **1.53**	*2078.97 m* **1.59** *2079.40 m* **1.20** *2100.6 m* **0.57**	–	–	*930–931 cm* **1.10**	–	–	**0.59**	–	–		–
		Askja (26%)	No match	–	–	–	–	–	–	–	–	–	–		–
		Katla (22%)	**SC**	–	–	–	–	–	–	*3173–3174 (pop 2)* **0.98**	–	–	–		–
			SD							*3173–3174 (pop 2)* **2.79**					
		WVZ/RVB (28%)	No match	–	–	–	–	–	–	–	–	–	–		–
Tephra zone 6: GS16-204-22CC, 266.25 cm		Grimsvötn (19%)	**SC**	–	–	–	*1713–1714 cm* **0.98**	–	–	–	–	–	–		–
			SD	–	–	–	*1713–1714 cm* **6.0**	–	–	–	–	–	–		–
		Veidivötn (39%)	No match	–	–	–	–	–	–	–	–	–	–		–
Tephra zone 7: GS16-204-22CC, 250–252 cm	150–500 µm	Veidivötn (88%)	No match	–	–	–	–	–	–	–	–	–	–		
	106–150 µm	Grimsvötn (71%)	No match	–	–	–	–	–	–	–	–	–	–		
Tephra zone 8: GS16-204-22CC, 226.25 cm		Katla (64%)	**SC**	*2079.4 m* **0.99**	*1929.95 m* **0.98**	*1677.6 m* **0.98**	*1680–1681 cm Table 1* **0.98**	–	–	–	–	–	–		–
			SD	*2079.40 m* **0.97**	*1929.95 m* **1.41**	*1677.6 m* **1.38**	*1680–1681 cm Table 1* **7.31**	–	–	–	–	–	–		–
		Veidivötn (20%)	No match	–	–	–	–	–	–	–	–	–	–		–
		Kverkfjöll (12%)	**SC**	–	–	–	–	*800–801 cm (THOL-2)* **0.98**	–	–	–	–	–		–
			SD	–	–	–	–	*800–801 cm (THOL-2)* **1.41**	–	–	–	–	–		–

(ca. 42.1 ± 0.5 ka b2k) were geochemically analysed for major elements. The results show a basaltic near-homogeneous geochemical population (Fig. 3A) indicating an affinity with the Veidivötn volcanic system in the EVZ (Harning *et al.*, 2018) (Fig. 4D,H). Veidivötn-type tephra does not appear in the Greenland ice-core records around that time (Bourne *et al.*, 2015). However, in a marine sediment core from the Goban Spur area [MD04-2820CQ, SW of Ireland (Fig. 1A)], a Veidivötn or Reykjanes tephra deposit was found at the Greenland stadial (GS) 12 to Greenland interstadial (GI) 11 transition (Abbott *et al.*, 2016). From the GICC05 chronology this transition is dated to 43.3 ka b2k (Rasmussen *et al.*, 2014). The Veidivötn tephra shards of this deposit represent a sub-population of a heterogeneous non-isochronous deposit (Abbott *et al.*, 2016). Statistical comparison between the geochemical analyses from MD04-2820CQ, 529–530 cm and TZ-4 results in an SC of 0.989 and an SD of 1.35, suggesting a clear geochemical match between both horizons in both sediment cores (Fig. 6B; Table 1). In addition, three Kverkfjöll shards from TZ-4 are geochemically similar to shards from an overlying peak in the same deposit (MD04-2820CQ, 524–525 cm), further supporting a link between the two deposits. The marine Goban Spur deposit is described as an ice-rafted tephra deposit with some reworked material, suggesting a delayed deposition following the volcanic eruption (Abbott *et al.*, 2016). By contrast, TZ-4 (ca. 42.4–42.1 ± 0.5 ka b2k) appears as a high-concentration peak with gradational up- and downward tailing of shards, indicative of a Type 2A deposit (Abbott *et al.*, 2018b). This tephra was probably deposited near-instantaneously by drifting sea ice and therefore is considered a potential useful isochron in future studies. Approximately 1000 years separate the Goban Spur (MD04-2820CQ, 529–530 cm) (Abbott *et al.*, 2016) horizon and TZ-4. Three possible explanations for this age discrepancy arise: (i) the deposits are from the same eruption, but deposition in the Goban Spur area was influenced by secondary transport mechanisms; (ii) the deposits represent two closely spaced eruptions from the same volcano; or (iii) the current age estimate for TZ-4 and/or the stratigraphic position from MD04-2820CQ, 529–530 cm, are inaccurate, and the two deposits are closer in time than the available data suggest.

Tephra zone 5 (TZ-5): GS16-204-22CC, 296.25–288.25 cm (ca. 39.4–38.7 ± 0.5 ka b2k)

Between 296.25 and 288.25 cm depth (ca. 39.4–38.7 ± 0.5 ka b2k, Supporting Information Fig. S2), elevated concentrations of tephra shards are observed (Fig. 2A,B). A first concentration peak is recorded at 296.25 cm (ca. 39.4 ± 0.5 ka b2k) and a second at 288.25 cm (ca. 38.7 ± 0.5 ka b2k). Geochemical analyses from both peaks show a heterogeneous basaltic composition (Fig. 3B) consisting of volcanic shards that can be affiliated with the Grímsvötn (EVZ), Askja (NVZ) and Katla (EVZ) volcanic systems according to Harning *et al.* (2018) (Fig. 5A,E; Table 1). TZ-5 occurs as two closely spaced peaks of increased tephra shards with a gradational tail on both sides, indicative of a Type 2B deposit (Abbott *et al.*, 2018b). The Askja shards do not match tephra layers recorded in either the Greenland ice-core records or the North Atlantic marine records (Bourne *et al.*, 2015; Voelker and Haflidason, 2015; Abbott *et al.*, 2018a). The Katla shards do geochemically match a sub-population of a non-isochronous tephra horizon from the Nordic Seas (MD99-2284, 3173–3174 cm, Horizon F, population 2; Berben *et al.*, 2020) (Fig. 6C; Table 1), which was deposited during GS-9 and stratigraphically fits with the layer described in this study. Nonetheless, as the MD99-2284, 3173–3174-cm horizon shows a heterogeneous geochemical composition and up- and downward tailing of shards, this deposit is considered to have been influenced by several secondary deposition mechanisms and an input of re-worked material (Berben *et al.*, 2020). Hence, it cannot be used as a time-parallel marker. In addition, the TZ-5 tephra shards assigned to the Grímsvötn volcanic system match several established horizons, as this system generated multiple ash deposits during this period, often grouped in marine ash zone FMAZ III. The FMAZ III ash zone was originally defined as a marine tephra deposit, but investigations in several Greenland ice-cores (Bourne *et al.*, 2013) detected tephra layers that fall within the broad geochemical compositional range of the marine FMAZ III. The results from the ice-cores indicated that the FMAZ III ash zone consists of several closely spaced eruption events, all of Grímsvötn volcanic type composition that could be separated and grouped by using minor variations in TiO_2 oxide content. Recently, a similar approach was attempted for a marine sediment core from the Nordic Seas (Berben *et al.*, 2020) that revealed, at least partially, a result similar to that obtained from the ice-cores. The TZ-5 Grímsvötn shards statistically match to three Grímsvötn-type eruptives which are recorded in the NGRIP ice-core (Bourne *et al.*, 2015) dating to the period 40.22–38.79 ka b2k (GI-9) (Table 1). The tephra shards from TZ-5 probably represent a mixture of these eruptives. When compared with the North Atlantic marine tephra framework, the Grímsvötn tephra shards are geochemically similar to two tephra populations identified by Abbott *et al.* (2018a): the GI-8 layer in MD04-2829CQ at 930–931 cm and the iceberg-rafted geochemical sub-population in GIK23415-9 at 302–306 cm (Fig. 1A), deposited during H4 (Fig. 6C; Table 1).

The TZ-5 tephra deposit coincides with increased IRD concentrations that represent H4 (Griem *et al.*, 2019). During H4, a collapse of adjacent continental ice sheets caused large amounts of icebergs to drift into the Labrador Sea. Hence, over a ca. 700-year time span (i.e. 296.25–288.25 cm) the tephra shards were probably transported in that manner, causing a delayed deposition. It is likely that the tephra-bearing icebergs originated from the IIS. Due to delayed deposition this deposit is not useful as a time-marker.

Regarding the geochemical signature of the TZ-5 deposit, the Katla shards geochemically match to a sub-population of a GS-9 deposit identified in the Nordic Seas (Berben *et al.*, 2020). Furthermore, TZ-5 contains tephra shards which geochemically resemble five identified Grímsvötn deposits in the time period between ca. 40 and 38 ka b2k, three of which are from the Greenland ice cores and two are marine deposits (Bourne *et al.*, 2015; Abbott *et al.*, 2018a). The latter are assigned to GI-8, while those in the ice-cores fall within GI-9. The TZ-5 Grímsvötn shards indicate a statistical match to all five of these deposits (Table 1), for which there are several possible explanations: (i) the age model from the marine deposits is off-set by one interstadial (ca. 2000 years) and the deposits were actually deposited closer in time than the current age model suggests; (ii) the marine and ice-core deposits represent two (or more) eruptions with very similar geochemistry, deposited in consecutive interstadials, and hence are not related; and (iii) the TZ-5 Grímsvötn shards were deposited after a delay due to iceberg transport which also captured shards from eruptions that occurred during GI-9 and GI-8, in which case the age model of GS16-204-22CC appears ~500 years too old [GI-8 (38.2 ka b2k; Rasmussen *et al.*, 2014)].

Tephra zone 6 (TZ-6): GS16-204-22CC, 266.25 cm (ca. 36.7 ± 0.5 ka b2k)

From level 266.25 cm (Fig. 2A,B) corresponding to ca. 36.7 ± 0.5 ka b2k (Supporting Information Fig. S2), basaltic

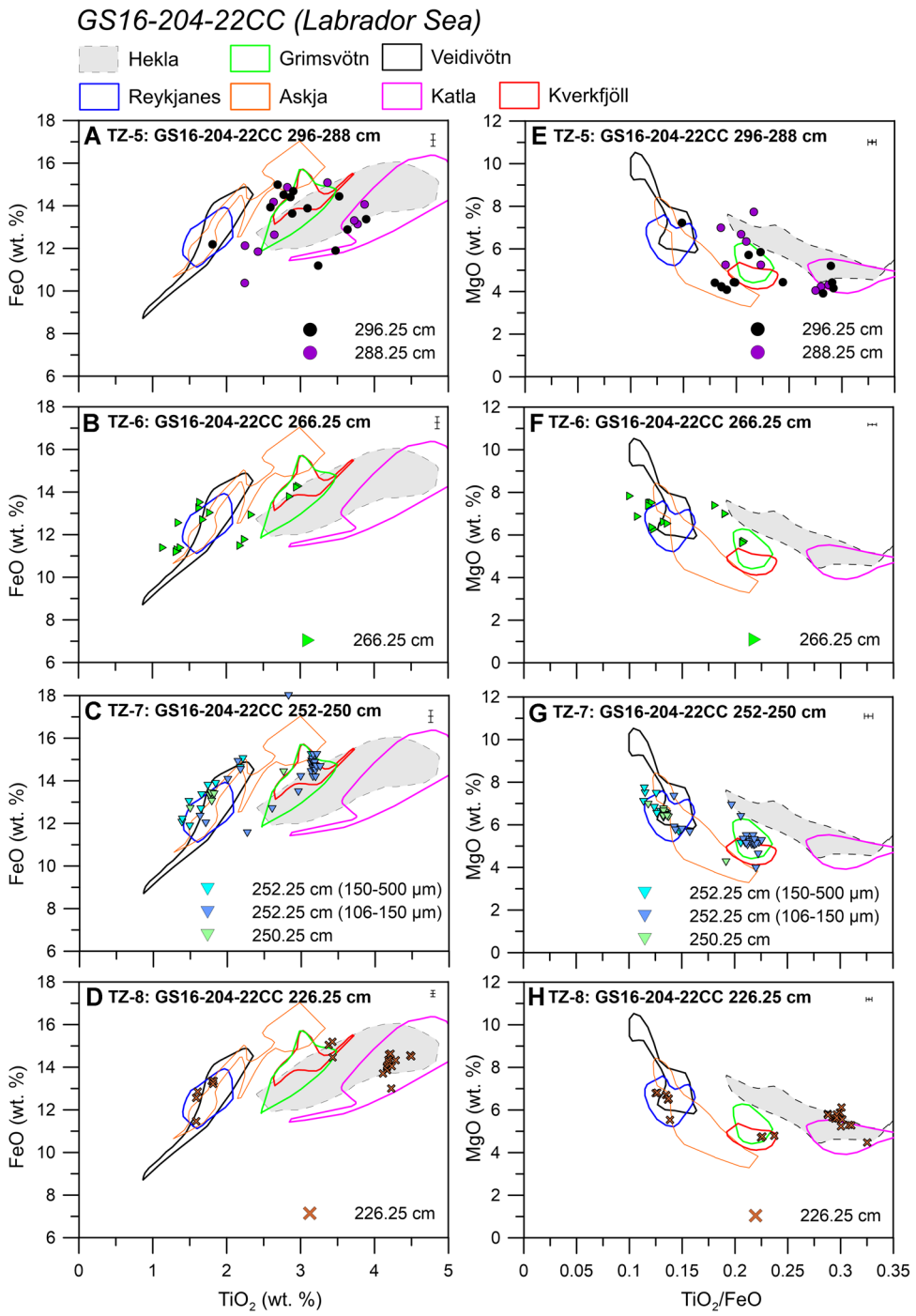

Figure 5. Visual biplot comparison (FeO versus TiO_2 and MgO versus TiO_2/FeO) of tephra shard analyses from marine sediment core GS16-204-22CC TZ 5–8. Geochemical envelopes of Icelandic volcanic systems are after Harning *et al.* (2018). Error bars represent two standard deviations of replicate analysis of BCR2g reference glass. [Color figure can be viewed at wileyonlinelibrary.com]

tephra shards (150–500 µm) were geochemically analysed. The analyses reveal a heterogeneous basaltic geochemistry (Fig. 3B) suggesting affinities to at least two different volcanic systems, Grímsvötn and Veidivötn (Harning *et al.*, 2018) (Fig. 5B,F; Table 1). There are no reports of Veidivötn eruptions around this time in either the North Atlantic marine records or the Greenland ice-core records (e.g. Wastegård *et al.*, 2006; Bourne *et al.*, 2015; Voelker and Haflidason, 2015; Abbott *et al.*, 2018a). However, the geochemistry of the Grímsvötn shards resembles that of a sub-population in core MD99-2251 [1713–1714 cm (THOL-1)] from the Reykjanes Ridge area (Fig. 1A) deposited before H3 (Abbott *et al.*, 2018a) (Fig. 6D; Table 1).

TZ-6 appears as one main tephra concentration peak with a downward tail of shards, probably caused by bioturbation, indicating a Type 3 deposit. The heterogeneous geochemical signature and evidence for increased IRD indicate a pulse of iceberg rafting. This transport mechanism is similar to that proposed for the geochemically matching sub-population in MD99-2251 (Abbott *et al.*, 2018a). Hence, deposition of TZ-6 was probably delayed and hence cannot serve as an isochronous marker.

Tephra zone 7 (TZ-7): GS16-204-22CC, 252.25–250.25 cm (ca. 34.8–34.5 ± 0.4 ka b2k)

A zone of basaltic tephra is observed within the interval 252–250 cm (Fig. 2A,B) (34.8–34.5 ± 0.4 ka b2k; Supporting Information Fig. S2a), which corresponds to a time span of ca.

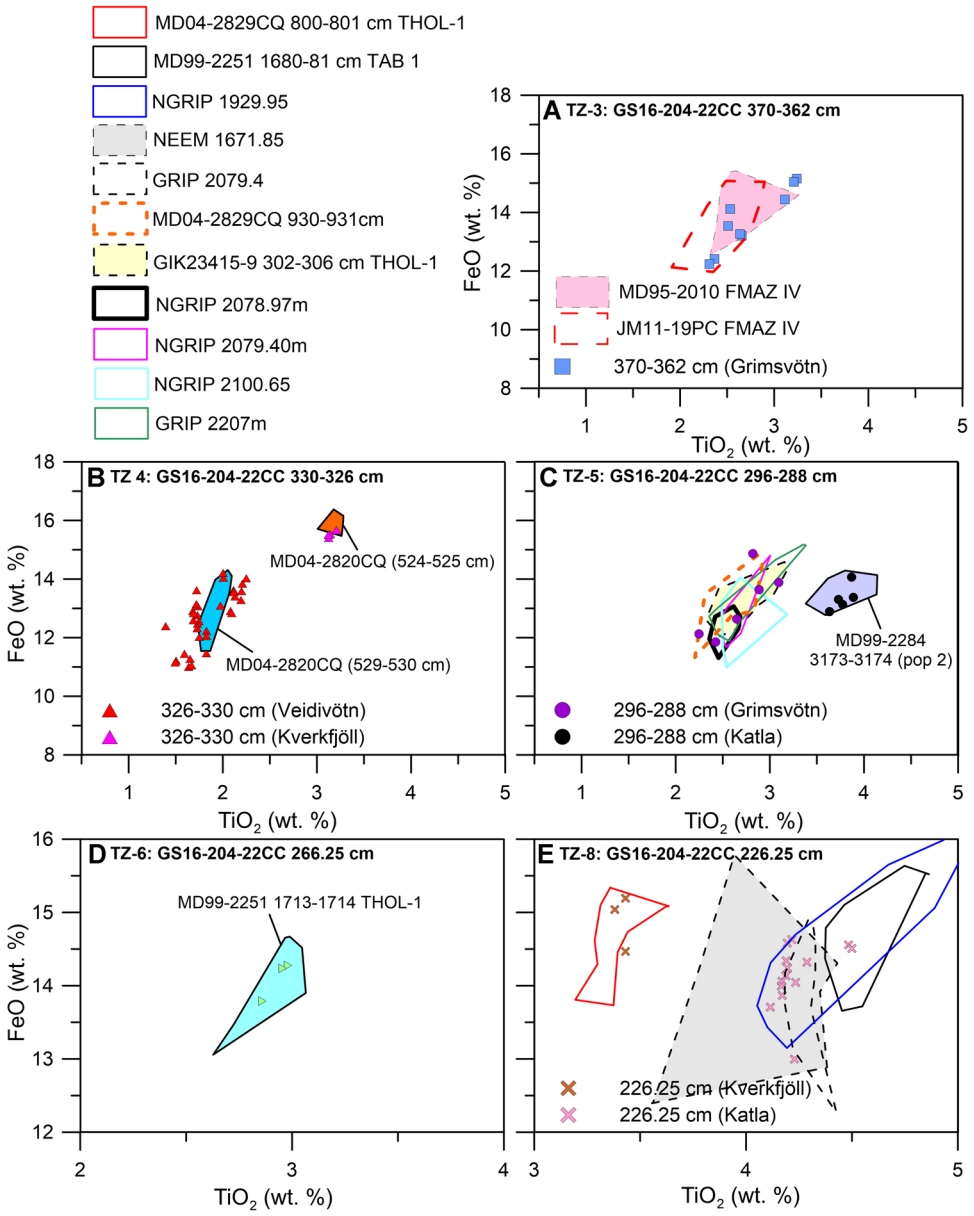

Figure 6. Visual biplot comparison of tephra shard analyses (major element oxides FeO and TiO_2) from tephra zones 3–6 and 8 in GS16-204-22CC to established tephra horizons. See Table 1 for references. [Color figure can be viewed at wileyonlinelibrary.com]

300 years. Within the analysed size fractions, the peak in the tephra concentration profile occurs at 252.25 cm (34.8 ± 0.4 ka b2k) (Fig. 2A,B). Nonetheless, basaltic shards from both 250.25 cm (34.5 ± 0.4 ka b2k, 150–500 µm) and 252.25 cm (34.8 ± 0.4 ka b2k, 150–500 and 106–150 µm) were geochemically analysed, to test for geochemical differences/similarities within the tephra zone. The analyses show two distinctly different populations: (i) within the coarse-grained size fraction (150–500 µm) a homogeneous geochemical population from the Veidivötn volcanic system (Harning *et al.*, 2018) is found between 252.25 and 250.25 cm; and (ii) within the fine-grained size fraction (106–150 µm), a homogeneous geochemical population (Fig. 3A) probably originating from the Grímsvötn volcanic system (Harning *et al.*, 2018) is observed (Fig. 5C,G). However, statistical analyses do not exclude Kverkfjöll as a potential alternative source. Neither of these tephra peaks geochemically match any previously established horizons within the Greenland ice-core records or the North Atlantic marine tephra framework (e.g. Wastegård *et al.*, 2006; Bourne *et al.*, 2015; Voelker and Haflidason, 2015; Abbott *et al.*, 2018a) (Table 1). Both the coarse- and the fine-grained deposits appear as one distinct tephra shard concentration peak, with some gradational upward and downward tailing consistent with a Type 2A deposit (Abbott *et al.*, 2018b). The deposit coincides with a small increase in IRD concentrations (Fig. 2C). It is therefore possible that the coarse-grained Veidivötn deposit was transported by sea ice rafting along the EGC, whereas the fine-grained Grímsvötn deposit is presumed to be of primary airborne material. Because both suggested transport mechanisms lead to near-instantaneous deposition of tephra, both peaks have the potential to serve as isochronous markers.

Tephra zone 8 (TZ-8): GS16-204-22CC, 226.25 cm (ca. 30.9 ± 0.4 ka b2k)

TZ-8 corresponds to a clear peak in the coarse-grained (150–500 µm) tephra shard concentration profile (Fig. 2A,B). Geochemical analyses of shards from this interval reveal a heterogeneous basaltic composition (Fig. 3B) indicating three possible volcanic sources: predominantly from the Katla volcanic system, but also from the Veidivötn and Kverkfjöll

volcanic systems (Fig. 5D,H; Table 1) (Harning *et al.*, 2018). The Veidivötn population does not match any established tephra horizon. The TZ-8 Katla population geochemically matches the Katla horizon identified in GRIP (2079.40 m), NGRIP (1929.95 m) and NEEM (1677.60 m) during GS-5.2 (31.4 ka b2k) yielding SCs between 0.98 and 0.99 and SDs between 0.97 and 1.41 (Fig. 6E; Table 1). In addition, TZ-8 geochemically matches the Katla isochron in MD99-2251 (1680–1681 cm, Table 1) (Abbott *et al.*, 2018a) deposited during H3. Furthermore, the TZ-8 Kverkfjöll shards geochemically resemble the MD04-2829CQ [800–801 cm (THOL-2)] (Fig. 1A) isochron (Fig. 6E; Table 1) from the eastern North Atlantic, deposited during GS-5.1 (Abbott *et al.*, 2018a). The TZ-8 tephra concentration profile shows a flat-bottom profile with an upward tailing of shards, indicating a Type 2B deposit (Abbott *et al.*, 2018b). The tephra deposit appears in conjunction with an IRD deposit which suggests iceberg rafting as the main transport agent. Thus, the deposit is not useful as an isochron. One of the populations is geochemically similar to a Katla eruption in the Greenland ice-core record that occurred around 31.4 ka b2k (Bourne *et al.*, 2015). If this was the source, it would imply a temporal delay of ~500 years between the Katla eruption in the Greenland ice-core record (Bourne *et al.*, 2015) and the deposition of the same material by icebergs in the Labrador Sea. The geochemical signature from a second population resembles a Kverkfjöll deposit identified in the eastern North Atlantic during the same time period (GS-5.1) (Abbott *et al.*, 2018a), but the two deposits were probably transported by different agents: near-instantaneous as suggested by Abbott *et al.* (2018a) and significantly delayed in the Labrador Sea (this study).

Discussion

Tephrochronological implications

We introduce five new tephra horizons with the potential to act as time-parallel markers for the Labrador Sea region in future studies. Four of the horizons originated from the Veidivötn volcanic system, whereas one was sourced from the Grimsvötn system. A summary of their key characteristics is provided in Table 2. These results suggest that although the prevailing wind-direction was probably eastwards (Haflidason *et al.*, 2000; Lacasse, 2001), tephra shards from Iceland were near-instantaneously deposited in marine sediment sequences located west of Iceland. Furthermore, four of the new tephra deposits identified in this study do not geochemically match established tephra horizons from either the North Atlantic marine tephra framework or the Greenland ice-core tephra lattice (e.g. Bourne *et al.*, 2013, 2015; Abbott *et al.*, 2016, 2018a). We propose that, after volcanic eruptions, the EGC rapidly transported Icelandic tephra material incorporated in the sea ice in a southward direction, to be deposited in southwestern regions of the North Atlantic. This mode of transportation might, however, confine deposition of these tephra layers to the Labrador Sea region, with little or no contemporaneous deposition to the east of Iceland, which have been the main focus area of previous marine North Atlantic marine tephra investigations.

The tephrostratigraphic record from core GS16-204-22CC is unique for both the area and the time period and offers the potential to make direct links between palaeoclimatic records from the Labrador Sea region and those from northern and eastern parts of the North Atlantic. However, this study has presented a continuous tephrostratigraphic record from the coarse-grained tephra fraction only, as examination of the fine-grained fraction was undertaken only for selected intervals. Hence, the full potential of the fine-grained ash component is not yet clear and should be the focus of future investigations.

Eruptive frequency of Icelandic volcanic systems during the LGP

Based on the tephrostratigraphic record from the Labrador Sea, we draw assumptions about the activity and eruptive frequency of several Icelandic volcanic systems during the LGP (Fig. 7). Throughout the record (65–30 ka b2k) the Veidivötn volcanic system consistently delivered material to the site, indicating that this system was very active during late MIS 4 and MIS 3. Before ca. 46 ka b2k, Torfajökull (NAAZ II-RHY-1) and Veidivötn appear to have been the only volcanic systems delivering material to the Labrador Sea. This is in line with previous studies that established an active Veidivötn system in MIS 4–5a, before the focused time interval of the present study (Brendryen *et al.*, 2010; Abbott *et al.*, 2011). However, in addition to Veidivötn, the Grímsvötn volcanic system was also active in the period before ca. 46 ka b2k, as shown by investigations in the northern Denmark Strait (Voelker and Haflidason, 2015). Potentially, at that time, this part of Iceland (i.e. the EVZ) was covered by less continental ice or by a retreating ice sheet, producing meltwater favourable for explosive eruptions (Larsen and Eiríksson, 2008). During MIS 3, more of the Icelandic volcanoes were active compared to the glacial conditions of MIS 4. This is also indicated by tephra records obtained from the Greenland ice-cores (Bourne *et al.*, 2015). In the early MIS 3 we record increased activity of the Grímsvötn and Kverkfjöll volcanic systems. Following this, at around 40 ka b2k, the eruptive activity of the Katla and Askja volcanic systems increased. Lastly, it is apparent that Hekla was not particularly active prior to the widespread eruption known as FMAZ II dated to around

Table 2. Overview of potential tephra time-parallel markers identified in this study with respect to their estimated age, deposition type, transport mechanism, volcanic system and geochemical match to established horizons.

Name of tephra horizon	Age (ka b2k)	Deposit type	Most likely transport mechanism	Match established horizon(s)?	Volcanic system
GS16-204-22CC, 530.25–524.25 cm	64.3–63.7 ± 0.5	Type 2A	Seasonal sea ice along the EGC	No	Veidivötn
GS16-204-22CC, 500.25 cm	58.1 ± 0.8	Type 2A	Seasonal sea ice along the EGC	No	Veidivötn
GS16-204-22CC, 330.25–326.25 cm	42.4–42.1 ± 0.5	Type 2A	Seasonal sea ice along the EGC	Yes, MD04-2829CQ (mixed)	Veidivötn
GS16-204-22CC, 252.25–250.25 cm (150–500 μm)	34.8–34.5 ± 0.4	Type 2A	Seasonal sea ice along the EGC	No	Veidivötn
GS16-204-22CC, 252.25 cm (106–150 μm)	34.8 ± 0.4	Type 2A	Primary airfall	No	Grímsvötn

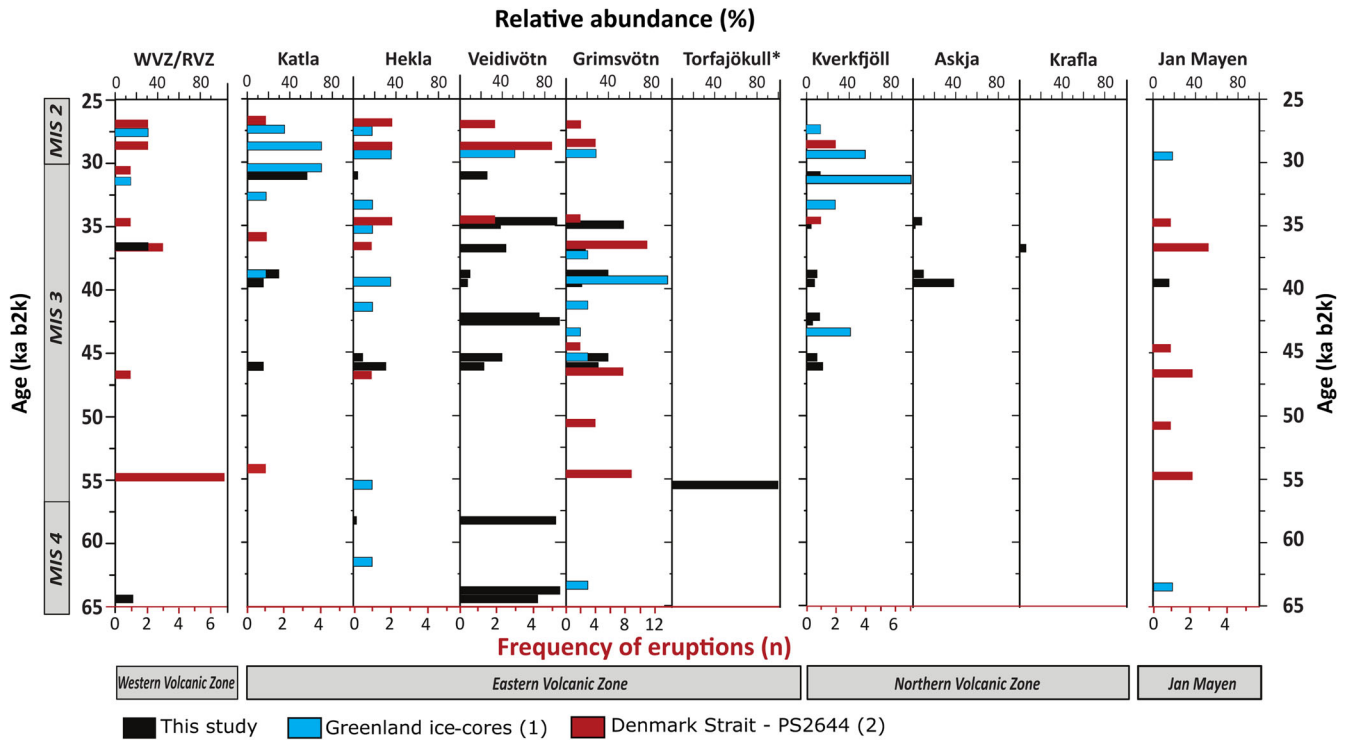

Figure 7. Estimated activity of selected Icelandic volcanoes based on the appearance in GS16-204-22CC (black bars), the Greenland ice-cores (blue bars) (Bourne *et al.*, 2013, 2015) and PS2644, Denmark Strait (red bars) (Voelker and Haflidason, 2015). Note that black bars show relative abundance in the analysed sample (%) that relate to the top *x*-axis, whereas blue and red bars follow the number of eruptions on the bottom *x*-axis. WVZ = Western Volcanic Zone, RVB = Reykjanes Volcanic Belt. *Based on results in Rutledal *et al.* (2020). [Color figure can be viewed at wileyonlinelibrary.com]

26.7 ka b2k (e.g. Haflidason *et al.*, 2000; Wastegård *et al.*, 2006; Davies *et al.*, 2008; Griggs *et al.*, 2014; Rutledal *et al.*, 2020).

The eruption sequences reflected in the Greenland ice-cores, marine core PS2644-5 and core GS16-204-22CC (Fig. 7) collectively suggest an eruption cyclicity of ca. 3–5 ka. This is most prominent for Veidivötn, but also in parts of the Grímsvötn record. This cyclical volcanic behaviour could reflect climate cycles that in turn modulated the volume of ice over Iceland, and/or changes in the transport pathway of ash to the Labrador Sea, Denmark Strait and Greenland. On that note, it is likely that the five primary deposits (TZ-1, -2, -4, -7 (106-150 µm and 150-500 µm), Table 2) reflect variability in the Icelandic eruptive frequency, while secondary deposits reflect changes in the transportation pathways to the Labrador Sea. Although intriguing, the proposed cyclicity needs to be substantiated by further, more detailed investigations, notably to establish the scale of delayed deposition of tephra by icebergs.

Conclusions

This first continuous stratigraphic record spanning the LGP from the Labrador Sea represents an initial stage in building a chronostratigraphic framework for this ocean sector. A total of eight tephra zones have been identified for the period 65–5 ka, five of which have the potential to serve as regional isochrons. However, at this point, these tephra isochrons do not geochemically match tephra horizons within the established North Atlantic tephra framework. The results show that the Veidivötn and Grímsvötn volcanic systems were most active during MIS 3. Prior to MIS 3 Veidivötn and Torfajökull were the only systems delivering material to the site. We find that the activity of the Veidivötn system during the studied interval shows a pattern of 3–5 ka cycles, which was also noted in the record for Grímsvötn tephras, although not through the whole core sequence. It is not clear if these cycles reflect variability in the frequency of eruptions from the volcanic systems or changes in the ice transport pathways and/or depositional mechanisms in the Labrador Sea.

Supporting information

Additional supporting information may be found in the online version of this article at the publisher's web-site.

Figure S1. Visual biplot comparison of the rhyolitic tephra shards identified at 130–130.5 cm (150–500 µm) compared to the Vedde Ash geochemical envelope.

Figure S2. Tephrostratigraphic record from Labrador Sea core GS16-204-22CC, 0–540 cm, versus age (ka b2k).

Table S1. Age control points in sediment core GS16-204-22CC.

Supporting information.

Acknowledgement. S.R., S.M.P.B., L.G. and E.J. have received funding from the European Research Council under the European Community's Seventh Framework Program (FP7/2007-2013)/ERC grant agreement 610055 as part of the ice2ice project. H.H. has received funding from the Research Council of Norway under NRC agreement 255415 as part of the CHASE project. We thank Dr. Chris Hayward for his assistance using the electron microprobe at the Tephra Analysis Unit, University of Edinburgh. We would also like to thank R/V G.O. Sars and the ice2ice GS16-204 cruise crew members for retrieving the material used in this study. We thank John Lowe and Peter M. Abbott for their comprehensive reviews which greatly improved the manuscript.

Data availability statement

The data that support the findings of this study are available in the Supporting Information.

Abbreviations. EGC, East Greenland Current; EPMA, electron-probe microanalysis; FMAZ, Faroe Marine Ash Zone; GI, Greenland Interstadial; GIS, Greenland Ice Sheet; GS, Greenland Stadial; IIS, Icelandic Ice Sheet; IRD, ice-rafted debris; LGM, Last Glacial Maximum; LGP, Last Glacial period; LIS, Laurentide Ice Sheet; MIS, Marine Isotope Stage; NAAZ, North Atlantic Ash Zone; RVB, Reykjanes Volcanic Belt; SC, similarity coefficient; SD, statistical distance; TZ, tephra zone; WGC, West Greenland Current; WVZ, Western Volcanic Zone.

References

Abbott PM, Bourne AJ, Purcell CS *et al*. 2016. Last glacial period cryptotephra deposits in an eastern North Atlantic marine sequence: exploring linkages to the Greenland ice-cores. *Quaternary Geochronology* **31**: 62–76.

Abbott PM, Davies SM, Austin WEN *et al*. 2011. Identification of cryptotephra horizons in a North East Atlantic marine record spanning marine isotope stages 4 and 5a (~60,000–82,000 a b2k). *Quaternary International* **246**: 177–189.

Abbott PM, Griggs AJ, Bourne AJ *et al*. 2018a. Tracing marine cryptotephras in the North Atlantic during the last glacial period: improving the North Atlantic marine tephrostratigraphic framework. *Quaternary Science Reviews* **189**: 169–186.

Abbott PM, Griggs AJ, Bourne AJ *et al*. 2018b. Tracing marine cryptotephras in the North Atlantic during the last glacial period: protocols for identification, characterisation and evaluating depositional controls. *Marine Geology* **401**: 81–97.

Batchelor CL, Margold M, Krapp M *et al*. 2019. The configuration of Northern Hemisphere ice sheets through the Quaternary. *Nature Communications* **10**: 3713.

Berben SMP, Dokken TM, Abbott PM *et al*. 2020. Independent tephrochronological evidence for rapid and synchronous oceanic and atmospheric temperature rises over the Greenland stadial-interstadial transitions between ca. 32 and 40 ka b2k. *Quaternary Science Reviews* **236**(106277). https://doi.org/10.1016/j.quascirev.2020.106277

Borchardt GA, Aruscavage PJ, Millard HTJR. 1972. Correlation of the Bishop Ash, a Pleistocene marker bed, using instrumental neutron activation analysis. *Journal of Sedimentary Petrology* **42**: 301–306.

Bourne AJ, Cook E, Abbott PM *et al*. 2015. A tephra lattice for Greenland and a reconstruction of volcanic events spanning 25–45 ka b2k. *Quaternary Science Reviews* **118**: 122–141.

Bourne AJ, Davies SM, Abbott PM *et al*. 2013. Revisiting the Faroe Marine Ash Zone III in two Greenland ice cores: implications for marine-ice correlations. *Journal of Quaternary Science* **28**: 641–646.

Brendryen J, Haflidason H, Sejrup HP. 2010. Norwegian Sea tephrostratigraphy of marine isotope stages 4 and 5: prospects and problems for tephrochronology in the North Atlantic region. *Quaternary Science Reviews* **29**: 847–864.

Davies SM. 2015. Cryptotephras: the revolution in correlation and precision dating. *Journal of Quaternary Science* **30**: 114–130.

Davies SM, Wastegård S, Rasmussen TL *et al*. 2008. Identification of the Fugloyarbanki tephra in the NGRIP ice core: a key tie-point for marine and ice-core sequences during the last glacial period. *Journal of Quaternary Science* **23**: 409–414.

Davis JO. 1985. Correlation of late Quaternary tephra layers in a long pluvial sequence near Summer Lake, Oregon. *Quaternary Research* **23**: 38–53.

Dokken TM, Cruise-Members. 2016. Ice2Ice Cruise GS16-204. In: Trond MD (ed.). Bjerknes Climate Data Centre.

Feyling-Hanssen, RF. 1971. Weichselian interstadial foraminifera from the Sandnes-Jæren area. *Bulletin of the Geological Society of Denmark* 21: 72–116.

Griem L, Voelker AHL, Berben SMP *et al*. 2019. Insolation and glacial meltwater influence on sea-ice and circulation variability in the northeastern Labrador Sea during the Last Glacial period. *Paleoceanography and Paleoclimatology* **34**: 1689–1709.

Griggs AJ, Davies SM, Abbott PM *et al*. 2014. Optimising the use of marine tephrochronology in the North Atlantic: a detailed investigation of the Faroe Marine Ash Zones II, III and IV. *Quaternary Science Reviews* **106**: 122–139.

Haflidason H, Eiriksson J, Kreveld SV. 2000. The tephrochronology of Iceland and the North Atlantic region during the Middle and Late Quaternary: a review. *Journal of Quaternary Science* **15**: 3–22.

Harning DJ, Thordarson T, Geirsdóttir Á *et al*. 2018. Provenance, stratigraphy and chronology of Holocene tephra from Vestfirðir, Iceland. *Quaternary Geochronology* **46**: 59–76.

Hayward C. 2012. High spatial resolution electron probe microanalysis of tephras and melt inclusions without beam-induced chemical modification. *The Holocene* **22**: 119–125.

Hesse R, Khodabakhsh S. 2016. Anatomy of Labrador Sea Heinrich layers. *Marine Geology* **380**: 44–66.

Kvamme T, Mangerud J, Furnes H *et al*. 1989. Geochemistry of Pleistocene ash zones in cores from the North Atlantic. *Norsk Geologisk Tidsskrift* **69**: 251–272.

Lacasse C. 2001. Influence of climate variability on the atmospheric transport of Icelandic tephra in the subpolar North Atlantic. *Global and Planetary Change* **29**: 31–55.

Lackschewitz KS, Wallrabe-Adams H-J. 1997. Composition and origin of volcanic ash zones in Late Quaternary sediments from the Reykjanes Ridge: evidence for ash fallout and ice-rafting. *Marine Geology* **136**: 209–224.

Larsen G, Eiríksson J. 2008. Late Quaternary terrestrial tephrochronology of Iceland – frequency of explosive eruptions, type and volume of tephra deposits. *Journal of Quaternary Science* **23**: 109–120.

Le Maitre RW, Bateman P. 1989. *A Classification of Igneous Rocks and Glossary of Terms: Recommendations of the International Union of Geological Sciences Subcommission on the Systematics of Igneous Rocks*. Blackwell Publishing: Oxford.

Lowe DJ. 2011. Tephrochronology and its application: a review. *Quaternary Geochronology* **6**: 107–153.

Pearce NJG, Alloway BV, Westgate JA. 2008. Mid-Pleistocene silicic tephra beds in the Auckland region, New Zealand: their correlation and origins based on the trace element analyses of single glass shards. *Quaternary International* **178**: 16–43.

Perkins ME, Nash WP, Brown FH *et al*. 1995. Fallout tuffs of Trapper Creek, Idaho—A record of Miocene explosive volcanism in the Snake River Plain volcanic province. *Geological Society of America Bulletin* **107**: 1484–1506.

Rasmussen SO, Bigler M, Blockley SP *et al*. 2014. A stratigraphic framework for abrupt climatic changes during the Last Glacial period based on three synchronized Greenland ice-core records: refining and extending the INTIMATE event stratigraphy. *Quaternary Science Reviews* **106**: 14–28.

Rutledal S, Berben SMP, Dokken TM *et al*. 2020. Tephra horizons identified in the western North Atlantic and Nordic Seas during the Last Glacial period: extending the marine tephra framework. *Quaternary Science Reviews* 240.

Svensson A, Andersen KK, Bigler M *et al*. 2008. A 60 000 year Greenland stratigraphic ice core chronology. *Climate of the Past* **4**: 47–57.

Thordarson T, Larsen G. 2007. Volcanism in Iceland in historical time: volcano types, eruption styles and eruptive history. *Journal of Geodynamics* **43**: 118–152.

Voelker AHL, Haflidason H. 2015. Refining the Icelandic tephrachronology of the last glacial period – the deep-sea core PS2644 record from the southern Greenland Sea. *Global and Planetary Change* **131**: 35–62.

Voelker , AHL, Sarnthein, M, Grootes, PM *et al*. 1998. Correlation of marine ^{14}C ages from the Nordic Seas with the GISP2 isotope record; implications for ^{14}C calibration beyond 25 ka BP. *Radiocarbon* **40**: 517–534.

Wastegård S, Rasmussen TL. 2014. Faroe Marine Ash Zone IV: a new MIS 3 ash zone on the Faroe Islands margin. In *Geological Society, London, Special Publication 398*, Austin WEN, Abbott PM, Davies SM, Pearce NJG, Wastegard S (eds). Geological Society of London: London.

Wastegård , S, Rasmussen, TL, Kuijpers, A *et al*. 2006. Composition and origin of ash zones from Marine Isotope Stages 3 and 2 in the North Atlantic. *Quaternary Science Reviews* **25**: 2409–2419. https://doi.org/10.1016/j.quascirev.2006.03.001

